Multiple Impedance Control for Space Free-Flying Robots

S. Ali A. Moosavian [*] **Rambod Rastegari** [†]

Department of Mechanical Engineering
K. N. Toosi Univ. of Technology
Tehran, Iran, P.O. Box 16765-3381
Email: moosavian@kntu.ac.ir

Evangelos Papadopoulos [‡]

Department of Mechanical Engineering
National Technical University of Athens
15780 Athens, Greece
Email: egpapado@central.ntua.gr

Abstract

To increase the mobility of on-orbit robotic systems, Space Free-Flying Robots (SFFR) in which one or more manipulators are mounted on a thruster-equipped base, have been proposed. Unlike fixed-based manipulators, the robotic arms of SFFR are dynamically coupled with each other and the free-flying-base, hence the control problem becomes more challenging. In this paper, the Multiple Impedance Control (MIC) is developed to manipulate space objects by multiple arms of SFFR. The MIC law is based on the concept of designated impedances and enforces them at various system levels, i.e., the free-flying base, all cooperating manipulators, and the manipulated object itself. The object may include an internal angular momentum source, as is the case in most satellite manipulation tasks. The disturbance rejection characteristic of this algorithm is also studied. The result of this analysis reveals that the effect of disturbances substantially reduces through

---

[*] Assistant Professor
† PhD Student
‡ Associate Professor, Member AIAA

appropriate tuning of the controller mass matrix gain. A system of three manipulators mounted on a free-flying base is simulated in which force and torque disturbances are exerted at several points. The system dynamics is developed symbolically and the controlled system is simulated. The simulation results reveal the merits of the MIC algorithm in terms of smooth performance, i.e. negligible small tracking errors in the presence of impacts due to contact with the obstacles and significant disturbances.

Nomenclature

$\mathbf{C}$	A vector which contains all gravity and nonlinear velocity terms of the dynamics model, where $\hat{\mathbf{C}}$ or $\tilde{\mathbf{C}}$ corresponds to the one in the task space, and a superscript "(i)" refers to the i-th manipulator.
$\mathbf{e}$, $\tilde{\mathbf{e}}$	Vector of tracking errors, where a subscript is used for a particular variable, e.g. $\mathbf{e}_\omega$ is the error in angular velocity, and a superscript "i" corresponds to the i-th manipulator.
$\mathbf{F}_c$	A 6×1 vector which contains the forces/moments applied on an acquired object due to contact with the environment.
$\hat{\mathbf{F}}_c$	Estimated value of contact force $\mathbf{F}_c$.
$\mathbf{F}_e$	A 6n×1 vector which contains all end-effector forces/torques applied on an acquired object, where $\mathbf{F}_e^{(i)}$ is a 6∞1 vector corresponding to the i-th end-effector.
$\mathbf{F}_{e_{req}}$	Required end-effector forces/torques to be applied on an acquired object, where $\mathbf{F}_{e_{req}}^{(i)}$ is a 6∞1 vector corresponding to the i-th end-effector.
$\mathbf{F}_G$	Required force for moving an internal angular momentum source along with the acquired object motion.
$\mathbf{F}_o$	A 6×1 vector which contains external forces/moments (other than contact and end-effector ones) applied on an acquired object.
$\mathbf{F}_\omega$	A 6×1 vector which contains nonlinear velocity terms in an acquired object dynamics equations.
$\mathbf{f}_c$, $\mathbf{n}_c$	Resultant force (torque) applied on an acquired object due to contact, where $\mathbf{n}_c$ includes moment of $\mathbf{f}_o$ about the object CM.
$\mathbf{f}_e^{(i)}$, $\mathbf{n}_e^{(i)}$	The i-th end-effector force (torque) exerted on an acquired object.
$\mathbf{f}_o$, $\mathbf{n}_o$	Vector of external forces (torques), other than contact and end-effector ones, applied on an acquired object (including gravity effects), where $\mathbf{n}_o$ includes moment of $\mathbf{f}_o$ about the object CM.
$\mathbf{G}$	A 6×6n grasp matrix which maps the vector of all end-effector forces/ torques to an acquired object dynamics equations.
$\mathbf{G}^\#$	A weighted pseudoinverse of the grasp matrix **G**.

$\mathbf{H}$	The positive definite mass matrix of the system, where $\hat{\mathbf{H}}$ or $\tilde{\mathbf{H}}$ corresponds to the one in the task space, and a superscript "i" refers to the i-th manipulator.
i_f	Number of applied force/torque vectors on a body.
$\mathbf{J}_C$	A square Jacobian matrix which relates the output speeds to the generalized ones, where a superscript "i" corresponds to the i-th manipulator..
$\mathbf{J}_Q$	An N×N Jacobian matrix which relates the vector of actuator forces/toques to the vector of generalized forces.
$\mathbf{J}_i^{(m)}$	A $6\times\mathbf{N}$ Jacobian matrix which relates the generalized velocities $\dot{\mathbf{q}}$ to the linear velocity ($\dot{\mathbf{R}}_i$) and angular velocity ($\boldsymbol{\omega}_i^{(m)}$) of the exerted body.
$\mathbf{K}_p$, $\mathbf{K}_d$	Control gain matrices.
$\mathbf{k}_e$	Stiffness matrix of an RCC unit.
$\tilde{\mathbf{k}}_p$, $\tilde{\mathbf{k}}_d$, $\tilde{\mathbf{M}}_{des}$	Block diagonal N×N control gain and desired mass matrices, composed of the corresponding 6×6 matrices which define the impedance law for the acquired object.
k_w	Stiffness coefficient of an obstacle located at x_w, in a unilateral study.
$\mathbf{L}_G$	Angular momentum of an internal source about the acquired object CM.
$\mathbf{L}_s$	Angular momentum of an internal source about its own CM.
$\mathbf{M}$	A 6×6 mass matrix for an acquired object.
$\mathbf{M}_{des}$	An acquired object desired mass matrix, in the impedance law.
$\mathbf{M}_G$	Required moment for moving an internal angular momentum source along with the acquired object motion.
m_{obj} , $\mathbf{I}_G$	An acquired object mass, and its moment of inertia about CM.
m_s	Mass of an internal angular momentum source which is not included in the acquired object mass m_{obj} .
n	Number of manipulators or appendages, for a system of multiple manipulators.
n_f	The number of disturbing torque/force applied on the i-th link of the m-th manipulator.
N	The system total degrees of freedom (DOF).
N_m	Number of joints (single DOF), for the m-th manipulator.
$\mathbf{p}_s$	Linear momentum of an internal angular momentum source, inside an acquired object.
$\mathbf{Q}$	Vector of generalized forces, where $\tilde{\mathbf{Q}}$ corresponds to the one in the task space, and a superscript "i" refers to the i-th manipulator.
$\tilde{\mathbf{Q}}_{app}$	Applied controlling force (expressed in the task space), where a superscript "i" refers to the i-th manipulator; $\tilde{\mathbf{Q}}_{app} = \tilde{\mathbf{Q}}_m + \tilde{\mathbf{Q}}_f$.
$\tilde{\mathbf{Q}}_f$	Required force to be applied on the manipulated object by the end-effector, where a superscript "i" refers to the i-th manipulator.
$\tilde{\mathbf{Q}}_m$	Applied controlling force concerning the motion of the end-effector, where a superscript "i" refers to the i-th manipulator.
$\tilde{\mathbf{Q}}_{react}$	Reaction force (expressed in the task space) on the end-effector, where a superscript "i" refers to the i-th manipulator.

$\mathbf{Q}_{dist_i\,j}^{(m)}$	The j-th disturbing torque/force applied on the i-th link of the m-th manipulator.
$\mathbf{Q}_{dist}$	Vector of generalized disturbing forces, where $\tilde{\mathbf{Q}}_{dist}$ corresponds to the one in the task space.
$\mathbf{q}$, $\dot{\mathbf{q}}$, $\ddot{\mathbf{q}}$	An N×1 vector of generalized coordinates, and its rate, where a superscript "i" corresponds to the i-th manipulator.
$\mathbf{R}_{C_0}$, $\dot{\mathbf{R}}_{C_0}$, $\ddot{\mathbf{R}}_{C_0}$	Inertial position, velocity, and acceleration of the spacecraft CM, where the components are expressed as x_0, y_0, z_0, etc.
$\mathbf{R}_{CM}$, $\dot{\mathbf{R}}_{CM}$, $\ddot{\mathbf{R}}_{CM}$	Inertial position, velocity, and acceleration of the system CM, where the components are expressed as x_{CM}, y_{CM}, z_{CM}, etc.
$\mathbf{r}_e^{(i)}$	The position vector of the i-th end-effector with respect to the object CM.
$\mathbf{r}_s$	Position vector of the angular momentum source CM with respect to the object CM.
$\mathbf{S}_{\text{obj}}$	A 3×3 matrix, which relates the angular velocity of an acquired object to the Euler angle rates.
$\mathbf{U}_{f_c}$	An N×6 matrix, composed of (n+1) 6×6 identity matrices.
$\mathbf{v}_s$	The inertial linear velocity of the internal angular momentum source CM.
$\mathbf{x}$	A 6×1 vector ($\mathbf{X} = (\mathbf{x}_G^T, \boldsymbol{\delta}_{obj}^T)^T$) which contains the CM position, and Euler angles of an acquired object, where $\dot{\mathbf{x}}$ and $\ddot{\mathbf{x}}$ are its rates, and $\mathbf{x}_{\text{des}}$, etc. are the desired ones.
$\tilde{\mathbf{x}}$, $\dot{\tilde{\mathbf{x}}}$, $\ddot{\tilde{\mathbf{x}}}$	A vector of controlled variables, and its rates, where $\tilde{\mathbf{x}}_{des}$, $\dot{\tilde{\mathbf{x}}}_{des}$, and $\ddot{\tilde{\mathbf{x}}}_{des}$ refer to the desired ones, and a superscript "i" corresponds to the i-th manipulator.
$\mathbf{x}_E^{(m)}$, $\dot{\mathbf{x}}_E^{(m)}$	The m-th end-effector inertial position, and velocity vector; $\mathbf{x}_E^{(m)} = (x_E{}^{(m)}, y_E{}^{(m)}, z_E{}^{(m)})$, etc.
$\mathbf{x}_G$, $\dot{\mathbf{x}}_G$, $\ddot{\mathbf{x}}_G$	Inertial position, velocity, and acceleration of an acquired object CM.
Δt	The time step used in the estimation procedure.
$\boldsymbol{\delta}_0$	A set of Euler angles which describes the spacecraft attitude; $\mathbf{d}_0 = (\alpha_0, \beta_0, \gamma_0)$.
$\boldsymbol{\delta}_E^{(m)}$	A set of Euler angles which describes the m-th end-effector orientation; $\boldsymbol{\delta}_E^{(m)} = (\alpha_E^{(m)}, \beta_E^{(m)}, \gamma_E^{(m)})$, and becomes a single angle $\delta_E{}^{(m)}$ in planar motion.
$\boldsymbol{\delta}_{obj}$	A set of Euler angles which describes an acquired object attitude.
$\boldsymbol{\theta}^{(m)}$	An N_m×1 column vector which contains the joint angles of the m-th manipulator, where $\theta_i{}^{(m)}$ refers to its i-th component (joint).
$\boldsymbol{\theta}$	A K×1 column vector which contains all joint angle vectors, $\left(\boldsymbol{\theta}^{(1)T}, \boldsymbol{\theta}^{(2)T}, \cdots, \boldsymbol{\theta}^{(n)T}\right)^T$.
${}^m\boldsymbol{\omega}_E^{(m)T}$	Angular velocity of the m-th end-effector expressed in its own body-fixed frame.
$\boldsymbol{\omega}_{obj}$, $\dot{\boldsymbol{\omega}}_{obj}$	An acquired object angular velocity, and acceleration.
$\mathbf{0}$	A zero matrix.
$\mathbf{1}$	The identity matrix.

1. Introduction

Robotic systems are expected to play an important role in space applications, e. g. in the servicing, construction, and maintenance of space structures on orbit. For instance, robotic systems may be used to inspect, capture, and repair or refuel damaged satellites. Ultimately, coordinated teams of robots might deploy, transport, and assemble structural modules for a large space structure[1]. Space Free-Flying Robots (SFFR) are robotic systems that include an actuated relatively small base equipped with one or more manipulators, Figure 1. Distinct from fixed-based manipulators, the base of SFFR responds to dynamic reaction forces due to manipulator motions. In order to control such a system, it is essential to consider the dynamic coupling between the manipulators and the base, by developing proper kinematics/dynamics model for the system[2-4]. Motion control of SFFR have been studied by various researchers[5-10]. Also, coordinated control of free-flying base and its multiple manipulators during capture or manipulation of objects has received attention[11-15].

In order to control interaction forces and system response during contact, force or impedance control strategies are required. *Hybrid position/force control* has been the basic strategy of several proposed implementations[16-17]. Nevertheless, due to several control mode switching during most tasks, particularly in unexpected situations, hybrid control does not provide an efficient interface. *Impedance Control* provides compliant behavior of a single manipulator in dynamic interaction with its environment[18]. An impedance controller enforces a relationship between external force(s)/torque(s) acting on the environment, and the position, velocity and acceleration error of the end-effector. Adaptive schemes have been presented to make impedance control capable of tracking a desired contact force, which has been described as the main shortcoming of impedance control in an unknown environment[19-20]. Optimizing the regulation of impedance control from the viewpoint of both the transient and steady state responses, using the concept of impedance matching to choose

optimal parameters has been proposed[21]. A Cartesian impedance controller has been presented to overcome the main problems encountered in fine manipulation, i.e. effects of the friction (and unmodeled dynamics) on robot performance and occurrence of singularity conditions[22-24]. Experimental and simulation investigations into the performance of impedance control implemented on elastic joints, have shown the benefits of using this control strategy in compensating undesirable effects due to system flexibilities[25].

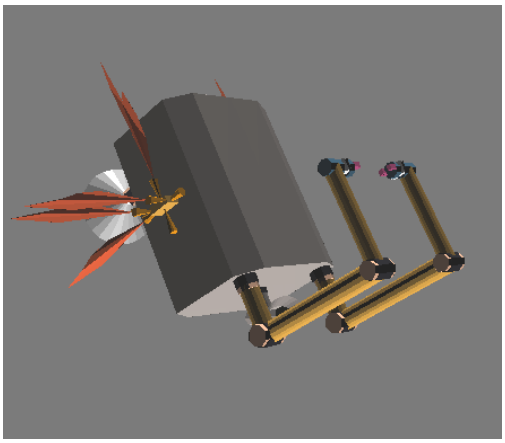

Fig. 1: A SFFR with multiple manipulators.

Object Impedance Control (OIC), has been developed for robotic arms manipulating a common object[26]. The OIC enforces a designated impedance not for an individual manipulator endpoint, but for the manipulated object itself. A combination of feedforward and feedback strategies is employed to make the object behave as a reference impedance. However, it has been recognized that applying the OIC to the manipulation of a flexible object may lead to instability[27]. It was suggested that either increasing the desired mass parameters or filtering the frequency content of the estimated contact force, may solve the instability problem. *Multiple Impedance Control (MIC)* is an algorithm that has been developed for several cooperating robotic systems manipulating a common object[28-29].

In this paper, the MIC law is studied in the context of space robotic systems. The MIC formulation is extended to impose a reference impedance to all elements of a SFFR, including its free-flying base, the manipulator end-points, and the manipulated object. It is assumed that the manipulated object includes an internal angular momentum source, as it is the case in most satellite manipulation tasks. The effect of torque/force disturbances applied on different points of the system is studied next. Results show that through appropriate tuning of the MIC mass matrix gain, the effect of disturbances is substantially reduced. Next, a system of three manipulators mounted on a space free-flyer is simulated during a planar maneuver. To consider practical aspects, it is assumed that a Remote Center Compliance is attached to the second end-effector, and that the system is subjected to significant force and torque disturbances at several points. Also, the desired trajectories are planned such that the object comes into a contact with an obstacle. Simulation results reveal the merits of the MIC algorithm in terms of its smooth performance, i.e. resulting in negligible small tracking errors in the presence of both impacts due to contact with the environment and imposed disturbances, and in a soft stop at the obstacle position following the contact.

2. The MIC Law for Space Free-Flyers

2.1. System Dynamics

In this section, a brief review of the dynamics modeling of space free-flying robots with multiple arms is presented, while for more details one should see Ref.[30] Assuming that the system consists of rigid elements, the vector of generalized coordinates can be chosen as

$$\mathbf{q} = \left({R_{CM}}^T, {\boldsymbol{\delta}_o}^T, \boldsymbol{\theta}^T \right)^T \tag{1}$$

where

$$\boldsymbol{\theta} = \left(\boldsymbol{\theta}^{(1)^T}, \cdots, \boldsymbol{\theta}^{(n)^T} \right)^T \tag{2}$$

which is a $\mathbf{K_n \times 1}$ column vector where $\boldsymbol{\theta}^{(\mathbf{m})}$ is an $\mathbf{N_m \times 1}$ column vector which contains the joint angles of m-th manipulator, and $K_n = \sum_{m=1}^{n} N_m$. The vector of output (controlled) variables is defined as

$$\tilde{\mathbf{X}} = \left[\mathbf{R}_{C_0}^T, \boldsymbol{\delta}_0^T, \mathbf{X}_E^{(1)T}, \boldsymbol{\delta}_E^{(1)T}, \cdots, \mathbf{X}_E^{(n)T}, \boldsymbol{\delta}_E^{(n)T} \right] \tag{3}$$

which is a $K_n + 6$ column vector. Applying the general Lagrangian formulation[31], or any other method, the equations of motion can be obtained and expressed in the task space, i.e. in terms of the output coordinates $\tilde{\mathbf{X}}$, as

$$\tilde{\mathbf{H}}(\mathbf{q})\ddot{\tilde{\mathbf{X}}} + \tilde{\mathbf{C}}(\mathbf{q}, \dot{\mathbf{q}}) = \tilde{\mathbf{Q}} \tag{4}$$

where $\tilde{\mathbf{H}}$ describes the system mass matrix, $\tilde{\mathbf{C}}$ contains all nonlinear terms, and $\tilde{\mathbf{Q}}$ describes the vector of generalized forces in the task space.

To develop the MIC law, the vector of generalized forces $\tilde{\mathbf{Q}}$, is written as

$$\tilde{\mathbf{Q}} = \tilde{\mathbf{Q}}_{app} + \tilde{\mathbf{Q}}_{react} = \tilde{\mathbf{Q}}_m + \tilde{\mathbf{Q}}_f + \tilde{\mathbf{Q}}_{react} \tag{5}$$

where $\tilde{\mathbf{Q}}_{\mathbf{react}}$ is the reaction force on the end-effectors, and $\tilde{\mathbf{Q}}_{\mathbf{app}}$ is the applied controlling force consisting of the force which corresponds to the motion of the system, $\tilde{\mathbf{Q}}_{\mathbf{m}}$, and of the required force to be applied on the manipulated object by the end-effectors, $\tilde{\mathbf{Q}}_{\mathbf{f}}$. To determine these terms, the object dynamics is considered next.

2.2. Object Dynamics

The equations of motion for a rigid object can be written as

$$\mathbf{M}\ddot{\mathbf{X}} + \mathbf{F}_{\boldsymbol{\omega}} = \mathbf{F}_c + \mathbf{F}_o + \mathbf{G}\mathbf{F}_e \tag{6}$$

An active object is assumed i.e. the object includes an internal angular momentum source, as shown in Figure 2. The above forces, the mass matrix **M**, and the *grasp matrix* **G** will be detailed in the following.

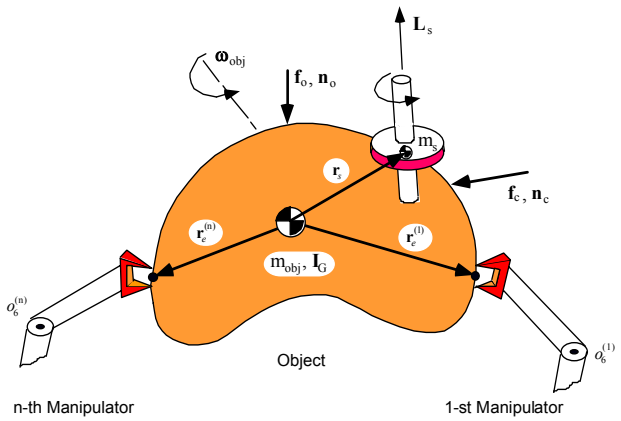

Fig. 2: An object with an internal angular momentum source, manipulated by cooperating manipulators.

The linear momentum of the source, $\mathbf{p}_s$, can be written as

$$\mathbf{p}_s = m_s \mathbf{v}_s = m_s (\dot{\mathbf{x}}_G + \boldsymbol{\omega}_{obj} \times \mathbf{r}_s) \tag{7}$$

The required force for moving the internal angular momentum source along with the object motion, $\mathbf{F}_G$, can be written as

$$\mathbf{F}_G = \dot{\mathbf{p}}_s = \frac{d}{dt} m_s \mathbf{v}_s \tag{8}$$

Therefore, differentiation of Eq. (7) and substitution of the result into Eq. (8), yields

$$\mathbf{F}_G = m_s \left(\ddot{\mathbf{x}}_G + \dot{\boldsymbol{\omega}}_{obj} \times \mathbf{r}_s + \boldsymbol{\omega}_{obj} \times (\boldsymbol{\omega}_{obj} \times \mathbf{r}_s) \right) \tag{9}$$

which has to be included in Eq. (6) for linear motion.

For the object angular motion, based on the *translation theorem* for angular momentum[31], it can be written

$$\mathbf{L}_G = \mathbf{L}_s + \mathbf{r}_s \times \mathbf{p}_s \tag{10}$$

Therefore, the required moment for moving the internal angular momentum source along with the object motion, written about the object center of mass is

$$\mathbf{M}_G = \dot{\mathbf{L}}_G + \dot{\mathbf{x}}_G \times \mathbf{p}_s \tag{11}$$

Assuming that $\mathbf{L}_s$ has a constant magnitude, results in

$$\mathbf{M}_G = \boldsymbol{\omega}_{obj} \times \mathbf{L}_s + \frac{d}{dt}\left(\mathbf{r}_s \times \mathbf{p}_s\right) + \dot{\mathbf{x}}_G \times m_s \left(\dot{\mathbf{x}}_G + \boldsymbol{\omega}_{obj} \times \mathbf{r}_s\right) \tag{12a}$$

Calculating different terms of Eq. (12), and substitution the results back into the equation, yields

$$\mathbf{M}_G = \boldsymbol{\omega}_{obj} \times \mathbf{L}_s + m_s \mathbf{r}_s \times \left(\ddot{\mathbf{x}}_G + \dot{\boldsymbol{\omega}}_{obj} \times \mathbf{r}_s + \boldsymbol{\omega}_{obj} \times (\boldsymbol{\omega}_{obj} \times \mathbf{r}_s)\right) \tag{12b}$$

which has to be included in Eq. (6) for angular motion, as

$$\begin{aligned} &\mathbf{I}_G \dot{\boldsymbol{\omega}}_{obj} + \boldsymbol{\omega}_{obj} \times \mathbf{I}_G \boldsymbol{\omega}_{obj} + \boldsymbol{\omega}_{obj} \times \mathbf{L}_s + m_s \mathbf{r}_s \times \left(\ddot{\mathbf{x}}_G + \dot{\boldsymbol{\omega}}_{obj} \times \mathbf{r}_s + \boldsymbol{\omega}_{obj} \times (\boldsymbol{\omega}_{obj} \times \mathbf{r}_s)\right) \\ &= \mathbf{n}_c + \mathbf{n}_o + \sum_{i=1}^{m} \mathbf{r}_e^{(i)} \times \mathbf{f}_e^{(i)} + \sum_{i=1}^{m} \mathbf{n}_e^{(i)} \end{aligned} \tag{13}$$

Now all these terms can be put together, and written in the matrix form of Eq. (6), where

$$\mathbf{M} = \begin{bmatrix} (m_{obj} + m_s)\mathbf{1}_{3\times 3} & -m_s [\mathbf{r}_s]^{\times} \mathbf{S}_{obj} \\ m_s \mathbf{S}_{obj}^T [\mathbf{r}_s]^{\times} & \mathbf{S}_{obj}^T (\mathbf{I}_G + \mathbf{I}_s) \mathbf{S}_{obj} \end{bmatrix} \tag{14a}$$

$$\mathbf{I}_s = m_s \begin{bmatrix} r_{s_y}^2 + r_{s_z}^2 & -r_{s_x} r_{s_y} & -r_{s_x} r_{s_z} \\ -r_{s_x} r_{s_y} & r_{s_x}^2 + r_{s_z}^2 & -r_{s_y} r_{s_z} \\ -r_{s_x} r_{s_z} & -r_{s_y} r_{s_z} & r_{s_x}^2 + r_{s_y}^2 \end{bmatrix} \tag{14b}$$

$$\mathbf{F}_c = \begin{Bmatrix} \mathbf{f}_c \\ \mathbf{S}_{obj}^T \mathbf{n}_c \end{Bmatrix} \quad \mathbf{F}_o = \begin{Bmatrix} \mathbf{f}_o \\ \mathbf{S}_{obj}^T \mathbf{n}_o \end{Bmatrix} \quad \mathbf{F}_e^{(i)} = \begin{Bmatrix} \mathbf{f}_e^{(i)} \\ \mathbf{n}_e^{(i)} \end{Bmatrix}_{6\times 1} \tag{14c}$$

$$\mathbf{F}_e = \begin{Bmatrix} \mathbf{F}_e^{(1)} \\ \vdots \\ \mathbf{F}_e^{(n)} \end{Bmatrix}_{6n\times 1} \tag{14d}$$

$$\begin{aligned} \mathbf{F}_{\boldsymbol{\omega}} = ((m_s \left[\boldsymbol{\omega}_{obj}\right]^{\times} \left[\boldsymbol{\omega}_{obj}\right]^{\times} \mathbf{r}_s - m_s \left[\mathbf{r}_s\right]^{\times} \dot{\mathbf{S}}_{obj} \dot{\boldsymbol{\delta}}_{obj})^T, (\mathbf{S}_{obj}^T (\left[\boldsymbol{\omega}_{obj}\right]^{\times} \mathbf{I}_G \boldsymbol{\omega}_{obj} + \left[\boldsymbol{\omega}_{obj}\right]^{\times} \mathbf{L}_s + \\ (\mathbf{I}_G + \mathbf{I}_s)\dot{\mathbf{S}}_{obj} \dot{\boldsymbol{\delta}}_{obj} + m_s \left[\mathbf{r}_s\right]^{\times} \left[\boldsymbol{\omega}_{obj}\right]^{\times} \left[\boldsymbol{\omega}_{obj}\right]^{\times} \mathbf{r}_s))^T)^T \end{aligned} \tag{14e}$$

$$\mathbf{G} = \begin{bmatrix} \mathbf{1}_{3\times 3} & \mathbf{0}_{3\times 3} & \cdots & \mathbf{1}_{3\times 3} & \mathbf{0}_{3\times 3} \\ \mathbf{S}_{obj}^T [\mathbf{r}_e^{(1)}]_{3\times 3}^{\times} & \mathbf{S}_{obj}^T & & \mathbf{S}_{obj}^T [\mathbf{r}_e^{(n)}]_{3\times 3}^{\times} & \mathbf{S}_{obj}^T \end{bmatrix}_{6\times 6n} \tag{14f}$$

where **1** and **0** denote the identity and zero matrices, respectively. The matrix $\mathbf{S}_{obj}$ relates the object angular velocity and the corresponding Euler rates as

$$\boldsymbol{\omega}_{obj} = \mathbf{S}_{obj} \dot{\boldsymbol{\delta}}_{obj} \tag{15}$$

It should be mentioned that for a flexible object an appropriate dynamics model can be simply substituted for the above model of a rigid object (Eq. (6)). Next, the MIC law is developed.

2.3. The MIC Law

A desired impedance law for the object motion can be chosen as

$$\mathbf{M}_{des} \ddot{\mathbf{e}} + \mathbf{K}_d \dot{\mathbf{e}} + \mathbf{K}_p \mathbf{e} = -\mathbf{F}_c \tag{16}$$

Then, considering the target impedance, the required end-effector forces/torques on the object are obtained using Eq. (6) as

$$\mathbf{F}_{e_{req}} = \mathbf{G}^{\#} \left\{ \mathbf{M} \mathbf{M}_{des}^{-1} \left(\mathbf{M}_{des} \ddot{\mathbf{X}}_{des} + \mathbf{K}_d \dot{\mathbf{e}} + \mathbf{K}_p \mathbf{e} + \mathbf{F}_c \right) + \mathbf{F}_{\boldsymbol{\omega}} - \left(\mathbf{F}_c + \mathbf{F}_o \right) \right\} \tag{17}$$

where $\mathbf{G}^{\#}$ is the pseudoinverse of the grasp matrix defined as

$$\mathbf{G}^{\#} = \mathbf{W}^{-1}\mathbf{G}^{T}\left(\mathbf{G}\mathbf{W}^{-1}\mathbf{G}^{T}\right)^{-1} \tag{18}$$

Therefore, the controlled forces $\tilde{\mathbf{Q}}_{\mathbf{f}}$ in Eq. (5) required to be applied on the manipulated object by the end-effectors is

$$\tilde{\mathbf{Q}}_{f} = \begin{Bmatrix} \mathbf{0}_{6\times 1} \\ \mathbf{F}_{e_{req}} \end{Bmatrix} \qquad \tilde{\mathbf{Q}}_{react} = \begin{Bmatrix} \mathbf{0}_{6\times 1} \\ -\mathbf{F}_{e} \end{Bmatrix} \tag{19}$$

where

$$\mathbf{F}_{e} = \mathbf{G}^{\#}\left[\mathbf{M}\ddot{\mathbf{X}} + \mathbf{F}_{\boldsymbol{\omega}} - \left(\mathbf{F}_{c} + \mathbf{F}_{o}\right)\right] \tag{20}$$

Next, to impose the same impedance law on the spacecraft motion, manipulators, and the object, the impedance law for the space free-flyer is written as

$$\tilde{\mathbf{M}}_{des}\ddot{\tilde{\mathbf{e}}}_{des} + \tilde{\mathbf{K}}_{d}\dot{\tilde{\mathbf{e}}} + \tilde{\mathbf{K}}_{p}\tilde{\mathbf{e}} + \mathbf{U}_{f_c}\mathbf{F}_{c} = \mathbf{0}_{N\times 1} \tag{21}$$

where $\tilde{\mathbf{e}} = \tilde{\mathbf{X}}_{des} - \tilde{\mathbf{X}}$ is the tracking error of the SFFR controlled variables (as opposed to "**e**" which describes the object tracking error) and $\tilde{\mathbf{M}}_{des}$, $\tilde{\mathbf{K}}_{p}$ and $\tilde{\mathbf{K}}_{d}$ are $N\times N$ block-diagonal matrices based on $\mathbf{M}_{des}$, $\mathbf{k}_{p}$ and $\mathbf{k}_{d}$ respectively, defined as

$$\tilde{\mathbf{M}}_{des} = \begin{bmatrix} \mathbf{M}_{des} & \mathbf{0} & \cdots & \mathbf{0} \\ \mathbf{0} & \mathbf{M}_{des} & \cdots & \vdots \\ \vdots & \mathbf{0} & \ddots & \mathbf{0} \\ \mathbf{0} & \cdots & \mathbf{0} & \mathbf{M}_{des} \end{bmatrix}_{\mathrm{N\times N}} \qquad \mathbf{U}_{f_c} = \begin{bmatrix} \mathbf{1}_{6\times 6} \\ \vdots \\ \mathbf{1}_{6\times 6} \end{bmatrix}_{\mathrm{N\times 6}} \tag{22a}$$

$$\tilde{\mathbf{K}}_{p} = \begin{bmatrix} \mathbf{k}_{p} & \mathbf{0} & \cdots & \mathbf{0} \\ \mathbf{0} & \mathbf{k}_{p} & \cdots & \vdots \\ \vdots & \mathbf{0} & \ddots & \mathbf{0} \\ \mathbf{0} & \cdots & \mathbf{0} & \mathbf{k}_{p} \end{bmatrix}_{\mathrm{N\times N}} \qquad \tilde{\mathbf{K}}_{d} = \begin{bmatrix} \mathbf{k}_{d} & \mathbf{0} & \cdots & \mathbf{0} \\ \mathbf{0} & \mathbf{k}_{d} & \cdots & \vdots \\ \vdots & \mathbf{0} & \ddots & \mathbf{0} \\ \mathbf{0} & \cdots & \mathbf{0} & \mathbf{k}_{d} \end{bmatrix}_{\mathrm{N\times N}} \tag{22b}$$

The desired trajectory for the system controlled variables, $\tilde{\mathbf{X}}_{des}$, can be defined based on the desired trajectory for the object motion, $\mathbf{X}_{des}$, and the grasp condition. Then, similar to the derivation for $\tilde{\mathbf{Q}}_f$ and assuming that the system mass and geometric parameters are known, $\tilde{\mathbf{Q}}_m$ can be obtained as

$$\tilde{\mathbf{Q}}_m = \tilde{\mathbf{H}}\tilde{\mathbf{M}}_{des}^{-1}\left[\tilde{\mathbf{M}}_{des}\ddot{\tilde{\mathbf{X}}}_{des} + \tilde{\mathbf{K}}_d\dot{\tilde{\mathbf{e}}} + \tilde{\mathbf{K}}_p\tilde{\mathbf{e}} + \mathbf{U}_{f_c}\mathbf{F}_c\right] + \tilde{\mathbf{C}} \tag{23}$$

Substituting these results into Eq. (5) makes all participating manipulators, the free-flyer-base, and the manipulated object exhibit the same impedance behavior, and guarantees an accordant motion of the various subsystems during object manipulation tasks. It should be noted that it was assumed that the exact value of the contact force is available, whereas usually substitution of an estimated value for this, as will be discussed later, is required. Also mass and geometric properties for the manipulated object, spacecraft and manipulating arms are known a reasonable assumption for space man-made systems. Finally, it should be mentioned that inspired by the human control system, a related formulation to fulfill desired force tracking tasks has been presented in Ref.[32].

2.4. Error Dynamics

In this section, error dynamics is studied to show that under the MIC law all participating manipulators, the free-flying base, and the manipulated object exhibit the same designated impedance behavior. Hence, an accordant motion of the manipulators and payload is achieved, and the MIC algorithm imposes a consistent motion of all parts of the system. To this end, substituting Eqs. (23) and (19) into Eq. (5), and the result into Eq. (4) yields

$$\tilde{\mathbf{H}}(\mathbf{q})\left(\tilde{\mathbf{M}}_{des}^{-1}\left(\tilde{\mathbf{M}}_{des}\ddot{\tilde{\mathbf{x}}}_{des} + \tilde{\mathbf{k}}_d\dot{\tilde{\mathbf{e}}} + \tilde{\mathbf{k}}_p\tilde{\mathbf{e}} + \mathbf{U}_{f_c}\mathbf{F}_c\right) - \ddot{\tilde{\mathbf{x}}}\right) + \begin{Bmatrix} \mathbf{0}_{6\times 1} \\ \mathbf{G}^{\#}\mathbf{M}\left(\mathbf{M}_{des}^{-1}\left(\mathbf{M}_{des}\ddot{\mathbf{x}}_{des} + \mathbf{k}_d\dot{\mathbf{e}} + \mathbf{k}_p\mathbf{e} + \mathbf{F}_c\right) - \ddot{\mathbf{x}}\right) \end{Bmatrix} = \mathbf{0} \tag{24}$$

Since Eq. (24) must hold for any $\mathbf{M}$ and $\tilde{\mathbf{H}}$, it can be concluded that

$$\begin{aligned}&\tilde{\mathbf{H}}(\mathbf{q})\left(\tilde{\mathbf{M}}_{des}^{-1}\left(\tilde{\mathbf{M}}_{des}\dddot{\tilde{\mathbf{x}}}_{des}+\tilde{\mathbf{k}}_d\ddot{\tilde{\mathbf{e}}}+\tilde{\mathbf{k}}_p\dot{\tilde{\mathbf{e}}}+\mathbf{U}_{f_c}\dot{\mathbf{F}}_c\right)-\ddot{\tilde{\mathbf{x}}}\right)=\mathbf{0}\\&\mathbf{G}^{\#}\mathbf{M}\left(\mathbf{M}_{des}^{-1}\left(\mathbf{M}_{des}\dddot{\mathbf{x}}_{des}+\mathbf{k}_d\ddot{\mathbf{e}}+\mathbf{k}_p\dot{\mathbf{e}}+\dot{\mathbf{F}}_c\right)-\ddot{\mathbf{x}}\right)=\mathbf{0}\end{aligned}\tag{25}$$

Now, based on Eqs. (14f) and (18) it can be seen that the pseudoinverse of the grasp matrix, $\mathbf{G}^{\#}$, is a full-rank matrix. Therefore, Eq. (25) results in

$$\begin{aligned}&\tilde{\mathbf{H}}(\mathbf{q})\left(\tilde{\mathbf{M}}_{des}^{-1}\left(\tilde{\mathbf{M}}_{des}\dddot{\tilde{\mathbf{x}}}_{des}+\tilde{\mathbf{k}}_d\ddot{\tilde{\mathbf{e}}}+\tilde{\mathbf{k}}_p\dot{\tilde{\mathbf{e}}}+\mathbf{U}_{f_c}\dot{\mathbf{F}}_c\right)-\ddot{\tilde{\mathbf{x}}}\right)=\mathbf{0}\\&\mathbf{M}\left(\mathbf{M}_{des}^{-1}\left(\mathbf{M}_{des}\dddot{\mathbf{x}}_{des}+\mathbf{k}_d\ddot{\mathbf{e}}+\mathbf{k}_p\dot{\mathbf{e}}+\dot{\mathbf{F}}_c\right)-\ddot{\mathbf{x}}\right)=\mathbf{0}\end{aligned}\tag{26}$$

Finally, based on the fact that $\mathbf{M}$ and $\tilde{\mathbf{H}}$ are positive definite inertia matrices, Eq. (26) results in

$$\begin{aligned}&\tilde{\mathbf{M}}_{des}\dddot{\tilde{\mathbf{e}}}_{des}+\tilde{\mathbf{K}}_d\ddot{\tilde{\mathbf{e}}}+\tilde{\mathbf{K}}_p\dot{\tilde{\mathbf{e}}}+\mathbf{U}_{f_c}\dot{\mathbf{F}}_c=\mathbf{0}\\&\mathbf{M}_{des}\ddot{\mathbf{e}}+\mathbf{K}_d\dot{\mathbf{e}}+\mathbf{K}_p\mathbf{e}+\mathbf{F}_c=\mathbf{0}\end{aligned}\tag{27}$$

Considering the definitions for $\tilde{\mathbf{M}}_{des}$, $\tilde{\mathbf{k}}_d$, $\tilde{\mathbf{k}}_p$, and $\mathbf{U}_{f_c}$ according to Eqs. (22), Eq. (27) means that all participating manipulators, the free-flyer-base, and the manipulated object exhibit the same impedance behavior. Next, the estimation procedure for the contact force is discussed.

2.5 Contact Force Estimation

As mentioned in the previous section, computation of $\mathbf{F}_{e_{req}}$ requires knowing the value of the contact force, $\mathbf{F}_c$. Normally, this has to be estimated which is discussed here.

Eq. (6) can be rewritten as

$$\mathbf{F}_c=\mathbf{M}\ddot{\mathbf{x}}+\mathbf{F}_{\boldsymbol{\omega}}-\mathbf{F}_o-\mathbf{G}\mathbf{F}_e\tag{28}$$

It is assumed that the external forces/torques $\mathbf{F}_o$, and also the object mass and geometric properties are known. Assuming that end-effectors are equipped with force sensors, $\mathbf{F}_e$ can be measured and substituted into Eq. (28). Also, based on the measurements of object motion, $\mathbf{F}_{\boldsymbol{\omega}}$ can be computed,

and substituted into Eq. (28). However, to evaluate the contact force, the object acceleration has to be known, too. Since this is not usually available, it has to be approximated through a numerical procedure. To implement Object Impedance Control, Schneider and Cannon (1992) suggest either to use the desired acceleration, or to use the last *commanded acceleration*, defined as

$$\ddot{\mathbf{x}}_{cmd} = \mathbf{M}_{des}^{-1}\left(\mathbf{M}_{des}\ddot{\mathbf{x}}_{des} + \mathbf{k}_d\dot{\mathbf{e}} + \mathbf{k}_p\mathbf{e} + \hat{\mathbf{F}}_c\right) \tag{29}$$

They describe that both of these two approximations yield acceptable experimental results, though it has been emphasized that a more sophisticated procedure would improve the performance. Since there may be a considerable difference between $\ddot{\mathbf{x}}$ and $\ddot{\mathbf{x}}_{des}$, particularly after contact, the first approach does not yield a reliable approximation. The second approach, may result in a poor approximation because of sudden variations at each contact.

Here, the approach taken is to use directly a finite difference approximation as

$$\hat{\ddot{\mathbf{x}}} = \frac{\dot{\mathbf{x}}_t - \dot{\mathbf{x}}_{t-\Delta t}}{\Delta t} \tag{30a}$$

or

$$\hat{\ddot{\mathbf{x}}} = \frac{\mathbf{x}_t - 2\mathbf{x}_{t-\Delta t} + \mathbf{x}_{t-2\Delta t}}{(\Delta t)^2} \tag{30b}$$

where Δt is the time step used in the estimation procedure. It should be mentioned that due to practical reasons (i.e. time requirement for measurements and corresponding calculations), Δt can not be infinitesimally close to zero. In practice, a sufficiently small Δt can be employed so that the resulting errors are negligible, even at the time of contact. Substituting Eq. (30) for acceleration, the contact force can be estimated from Eq. (28) as

$$\hat{\mathbf{F}}_c = \mathbf{M}\hat{\ddot{\mathbf{x}}} + \mathbf{F}_{\boldsymbol{\omega}} - \mathbf{F}_o - \mathbf{G}\mathbf{F}_e \tag{31}$$

Next, the disturbance rejection characteristics of the MIC algorithm are studied.

3. Disturbance Rejection Analysis

The effects of disturbances that are applied on several arbitrary points of a SFFR are considered here. The resultant generalized disturbance can be described as[33]

$$\mathbf{Q}_{dist} = -\sum_{j=1}^{n_f} \mathbf{J}_i^{(m)^T} \mathbf{Q}_{dist_i\, j}^{(m)} \tag{32}$$

where the Jacobian matrix $\mathbf{J}_i^{(m)}$ is a $6\times\mathbf{N}$ matrix defined as

$$\begin{Bmatrix} \dot{\mathbf{R}}_i \\ \boldsymbol{\omega}_i^{(m)} \end{Bmatrix} = \mathbf{J}_i^{(m)} \dot{\mathbf{q}} \tag{33}$$

which relates the generalized velocities $\dot{\mathbf{q}}$ to the linear velocity ($\dot{\mathbf{R}}_i$) and angular velocity ($\boldsymbol{\omega}_i^{(m)}$) of the exerted body. The generalized disturbance as described in Eq. (32) in the joint space, can be expressed in the task space as

$$\tilde{\mathbf{Q}}_{dist} = \left(\mathbf{J}_c^T\right)^{-1} \mathbf{Q}_{dist} \tag{34}$$

where the Jacobian matrix $\mathbf{J}_c$ is defined as

$$\dot{\tilde{\mathbf{X}}} = \mathbf{J}_c \dot{\mathbf{q}} \tag{35}$$

Therefore, the vector of generalized forces in the task space, $\tilde{\mathbf{Q}}$, as given in Eq. (5) will be obtained as

$$\tilde{\mathbf{Q}} = \tilde{\mathbf{Q}}_m + \tilde{\mathbf{Q}}_f + \tilde{\mathbf{Q}}_{react} + \tilde{\mathbf{Q}}_{dist} \tag{36}$$

Noting the fact that $\tilde{\mathbf{Q}}_f$ is virtually canceled by the reaction load on each end-effector, $\tilde{\mathbf{Q}}_{react}$, and substituting Eq.(36) into Eq. (4) it is obtained

$$\tilde{\mathbf{H}}(\mathbf{q})\ddot{\tilde{\mathbf{X}}} + \tilde{\mathbf{C}}(\mathbf{q}, \dot{\mathbf{q}}) = \tilde{\mathbf{Q}}_m + \tilde{\mathbf{Q}}_{dist} \tag{37}$$

Next, substituting Eq. (23) into Eq. (37) it can be obtained

$$\tilde{\mathbf{H}}(\mathbf{q})\,\tilde{\mathbf{M}}_{des}^{-1}\left[\tilde{\mathbf{M}}_{des}\,\ddot{\tilde{\mathbf{X}}}_{des}+\tilde{\mathbf{K}}_{d}\,\dot{\tilde{\mathbf{e}}}+\tilde{\mathbf{K}}_{p}\,\tilde{\mathbf{e}}+\mathbf{U}_{f_c}\,\mathbf{F}_{c}\right]+\tilde{\mathbf{C}}(\mathbf{q},\dot{\mathbf{q}})+\tilde{\mathbf{Q}}_{dist}=\tilde{\mathbf{H}}(\mathbf{q})\,\ddot{\tilde{\mathbf{X}}}+\tilde{\mathbf{C}}(\mathbf{q},\dot{\mathbf{q}}) \tag{38}$$

which can be simplified to

$$\tilde{\mathbf{M}}_{des}\,\ddot{\tilde{\mathbf{e}}}_{des}+\tilde{\mathbf{K}}_{d}\,\dot{\tilde{\mathbf{e}}}+\tilde{\mathbf{K}}_{p}\,\tilde{\mathbf{e}}+\mathbf{U}_{f_c}\,\mathbf{F}_{c}=-\tilde{\mathbf{M}}_{des}\tilde{\mathbf{H}}^{-1}(\mathbf{q})\tilde{\mathbf{Q}}_{dist} \tag{39}$$

As it is seen, the resultant disturbing torque/force appears in the right hand side of the whole system error equation. Noting the fact that the inertia matrix $\tilde{\mathbf{H}}(\mathbf{q})$ is a positive definite matrix, it can be guaranteed that $\tilde{\mathbf{H}}^{-1}(\mathbf{q})$ remains bounded. As expected from physical intuition, Eq. (39) reveals that increasing the mass properties of SFFR reduces the effects of disturbances. Also, the desired mass matrix appears as a coefficient in the right hand side of Eq. (39). This means that one can reduce the effects of disturbances by choosing lower values for the elements of $\tilde{\mathbf{M}}_{des}$. It should be noted that by decreasing the values for the elements of $\tilde{\mathbf{M}}_{des}$, the system behaves with lower inertia and its response becomes faster.

Next, to examine the developed MIC law, a system of three appendages mounted on a space free-flyer is simulated.

4. Simulation Results

As shown in Figure 3, a system of two manipulators mounted on a space free-flyer is simulated in this Section, in which a third appendage is considered as a communication antenna. A Remote Center Compliance (RCC) is attached to the second end-effector, Figure 3, to consider practical aspects (see Ref.[34]), and also to show the capability of MIC law in the presence of system flexibility. The SFFR performs a cooperative manipulation task**,** i.e. moving an object with two manipulators according to predefined trajectories, and is subject to significant force and torque disturbances at several points. As

shown in Figure 3, the antenna is connected to the base of the system and should keep a constant absolute orientation toward a remote center. For illustration purposes, the desired trajectory for the object is planned such that passes through an obstacle, and the object has to come to a smooth stop at the obstacle. The object has been grabbed with a pivoted grasp condition, i.e. no torque can be exerted on the object by the two end-effectors. The initial conditions, and system geometric parameters, mass properties, and the maximum available actuator torques and forces of system base, antenna, cooperative manipulators and manipulated object has been presented in the Appendix.

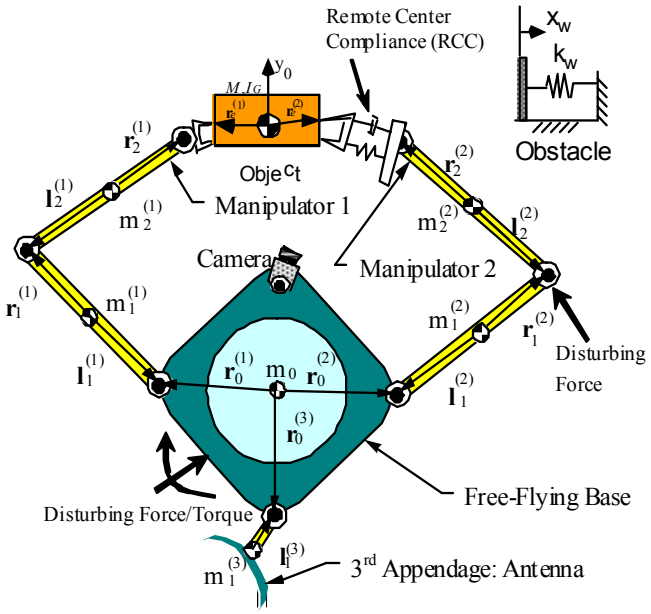

Fig 3. The simulated SFFR performing a cooperative object manipulation task, under the effect of disturbing forces/torques.

The system dynamics model of the described SFFR, which is a central element in the simulation code, using a barycentric method, and MAPLE tools. The code (SPACEMAPLE) yields the mass matrix **H**, the vector of nonlinear velocity terms **C** (both in the joint space and task space), also the Jacobian matrix and its time derivative, each one as an analytical function of generalized coordinates and speeds[30]. Next, the dynamics model in a symbolic (analytical) format is imported to the

simulation routine in MATLAB, where equations of motion under the developed MIC law are integrated, using the Gear algorithm.

The obstacle is at x_w=3.1m, so it is expected that the object will come into contact at its right side. Therefore, as seen in the following simulation results, the contact occurs at $t \approx 7.5$ s along x-direction, so that no contact force does affect the object motion in the y-direction. After the contact, since the x-position depends on the dynamics of the environment, according to the impedance law, the base smoothly comes back until position converges to a final value, which is determined by the desired contact force on the obstacle. It is assumed that no torque is developed at the contact surface (i.e. a point contact occurs), therefore $\mathbf{n}_c$ is equal to the moment of $\mathbf{f}_c$. Also, there is no other external force applied on the object, i.e. $\mathbf{f}_o = \mathbf{0}, \mathbf{n}_o = \mathbf{0}$. The contact force is calculated based on the real stiffness of the obstacle, which is $k_w = 1e5\ N/m$. The desired trajectories for the object and base center of mass, expressed in the inertial frame, are chosen as

$$x_{des_o} = -0.1791 + 4\left(1 - e^{-0.2t}\right) \quad (m) \qquad x_{des_{base}} = 0.025 + 3\left(1 - e^{-0.2t}\right) \quad (m)$$
$$y_{des_o} = 0.4 \quad (m) \qquad y_{des_{base}} = -0.03 \quad (m)$$

where the origin of the inertial frame is considered to be located at the system center of mass at initial time.

The controller gains are chosen as

$$\mathbf{K}_p = diag(100,...,100)\ \ (Kg\,S^{-2}) \quad \& \quad \mathbf{K}_d = diag(20,...,20)\ \ (Kg\,S^{-1})$$

First, to see the effect of mass matrix gain on the system behavior, no disturbances are considered and the system performance is simulated in three cases, i.e. different selections of the desired mass matrix $\mathbf{M}_{des} = diag(1,...,1)$, $\mathbf{M}_{des} = diag(0.5,...,0.5)$, and $\mathbf{M}_{des} = diag(0.2,...,0.2)$. As shown in Figure 4, by decreasing the values of controller mass matrix elements, the y-component of the object position

tracking error remains very close to zero before the contact, and eventually vanishes after that. Note that the contact occurs along x-direction, at $t \approx 7.5$ s, so that does not affect the object motion in the y-direction. It should be mentioned that other position tracking errors, i.e. free-flying base and the two manipulators end-effectors, are very similar to the object position tracking errors. Also, decreasing the values of controller mass matrix elements, has similar effect on the rate of these errors and results in a smoother tracking. Consequently, the contact force estimation procedure, which is based on finite difference calculation of the object acceleration, yields more accurate results. Therefore, as shown in Figure 4, when no disturbances are applied on the system, decreasing the values of controller mass matrix elements has minor improving effects on the system performance.

To see disturbance rejection characteristics for the developed MIC law, disturbing forces/torques of step type equal to [50 N, 50 N, 50 N.m] are applied on the free-flyer base at a distance of [0.5, 0.5] in its body coordinate, when it reaches to $x = 1.5m$ in the inertial frame. Another disturbing force equal to [50 N,50 N] is applied on the second joint of the second manipulator, as depicted in Figure 3. Note that these disturbances are significant, compared to the base actuator saturation limits. The system performance is now simulated for the two selections of $\mathbf{M}_{des} = diag(0.15,...,0.15)$ and $\mathbf{M}_{des} = diag(1.0,...,1.0)$, and the results are depicted in Figure 5.

As shown in Figure 5a, the y-component of the object position tracking error remains very close to zero before the contact, and eventually vanishes after that. This is due to the fact that the contact occurs along x-direction, so that it does not affect the object motion in the y-direction. Other position tracking errors, i.e. free-flying base position errors and manipulator end-effectors, and the rate of these errors behave similarly to the object position tracking errors. On the other hand, the x-component of error, starting from some initial value, decreases at some rate till contact occurs, at $t \approx 7.5$ s, Fig. 5. This rate changes after contact, because the tracking error dynamics depends on the

dynamics of the environment, according to the impedance law. Then, this error smoothly converges to the distance between the final desired x-position and the obstacle x-position.

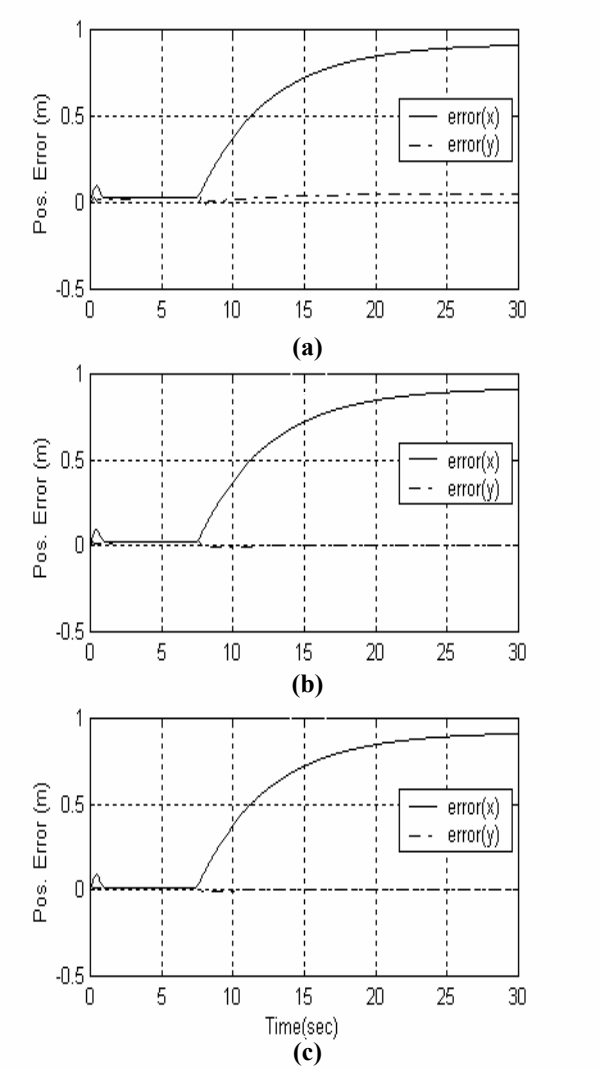

Fig. 4: Object Position Tracking Error when no Disturbing Forces/ Torques are applied: (a) $\mathbf{M}_{des} = diag(1,...,1)$**, (b)** $\mathbf{M}_{des} = diag(0.5,...,0.5)$**, (c)** $\mathbf{M}_{des} = diag(0.2,...,0.2)$**.**

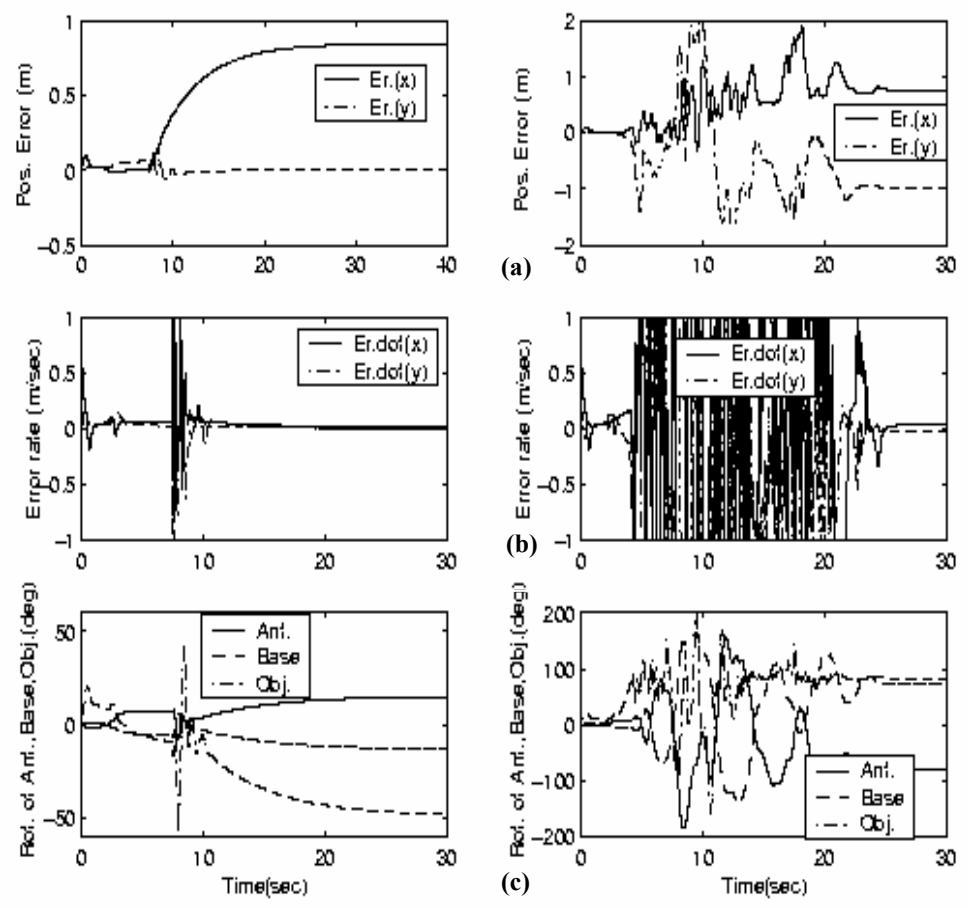

Fig. 5: Disturbing Forces/ Torques are applied on the Base and Manipulator: $\mathbf{M}_{des} = diag(0.15,...,0.15)$ (left), and $\mathbf{M}_{des} = diag(1.0,...,1.0)$ (Right): (a) Object Position Tracking Error, (b) Tracking Error Rates, (c) Orientation Tracking Error.

As discussed in previous section, decreasing the values of controller mass matrix has a substantial effect on the error dynamics. As seen in Figure 5, lower values of controller mass matrix elements (corresponding to the left hand side of the figure) result in smaller object tracking error, and so does on other position tracking errors. The orientation error starting from zero grows to some amount until contact occurs and then, it converges to a final limited value. The initial growth is due to the fact that the first end-effector (i.e. without the RCC unit) responds faster than the second one. Therefore, the difference between the two end-effector forces produces some couples that results in an undesirable

rotation of the object. Since there is no direct control on the object orientation, due to the pivoted grasp condition, the object orientation converges to a final limited value. As seen in Figure 5, the object position error and its time derivative, also other errors in rotation of base, antenna and all manipulator end-effectors decrease by reducing the values of desired mass matrix. The simulation results reveal the merits of the MIC algorithm in terms of suitably smooth performance, i.e. proper tracking errors in the presence of impacts due to contact with the obstacle and also significant disturbances.

5. Conclusions

In this paper, the MIC law was formulated and applied to space robotic systems. In space, participating robotic arms are connected through a free-flying-base, and the formulation had to consider the dynamic coupling between the arms and the base. For the manipulated object, inclusion of an internal source of angular momentum was admitted, as is the case for most satellite manipulation tasks. By error analysis, it was shown that under the MIC law, all participating manipulators, the free-flyer base, and the manipulated object exhibit the same designed impedance behavior. Next, the disturbance rejection characteristics of the MIC law applied to a SFFR in manipulating an object was studied. It was shown that increasing the mass properties of SFFR, which is an inherent characteristic of the system, reduces the effects of disturbances. It was also shown that the effect of disturbances can be substantially decreased by appropriate tuning of the controller mass matrix gain. Finally, to examine the developed MIC law, a system of three appendages mounted on a space free-flyer was simulated. Based on the simulation results the merits of the MIC algorithm in terms of disturbance rejection characteristics was revealed, i.e. negligible small tracking errors can be achieved in the presence of significant disturbing forces/torques. This is due to the fact that based on the MIC law all participating manipulators, the free-flyer-base, and the manipulated object exhibit the

same impedance behavior, which guarantees an accordant motion of the various subsystems during object manipulation tasks.

References

[1]Jacobsen, S., Lee, C., Zhu, C., and Dubowsky, S., "Planning of Safe Kinematic Trajectories for Free Flying Robots Approaching an Uncontrolled Spinning Satellite," *Proc. Of ASME 2002 Design Engineering Technical Conferences*, Montreal, Canada, 2002.

[2]Vafa, Z. and Dubowsky, S., "On The Dynamics of Manipulators in Space Using The Virtual Manipulator Approach," *Proc. of IEEE Int. Conf. on Robotics and Automation*, Raleigh, NC, 1987, pp. 579-585.

[3]Xu, Y., "The Measure of Dynamic Coupling of Space Robot Systems," *Proc. of IEEE Int. Conf. on Robotics and Automation*, Atlanta, Georgia, 1993, pp. 615-620

[4]Moosavian, S. Ali A. and Papadopoulos, E., "On the Kinematics of Multiple Manipulator Space Free-Flyers and Their Computation," *Journal of Robotic Systems*, Vol. 15, No. 4, 1998, pp. 207-216.

[5]Moosavian, S. Ali. A. and Papadopoulos, E., "Coordinated Motion Control of Multiple Manipulator Space Free-Flyers," *Proc. of the 7th AAS/ AIAA Space Flight Mechanics Meeting*, Huntsville, Al., USA, February 10-12, 1997.

[6]Umetani, Y. and Yoshida, K., "Resolved Motion Control of Space Manipulators with Generalized Jacobian Matrix," *IEEE Trans. on Robotics and Automation*, Vol. 5, No. 3, 1989, pp. 303-314.

[7]Alexander, H. and Cannon, R., "An Extended Operational Space Control Algorithm for Satellite Manipulators," *The Journal of the Astronautical Sciences*, Vol. 38, No. 4, 1990, pp. 473-486.

[8]Dubowsky, S. and Papadopoulos, E., "The Dynamics and Control of Space Robotic Systems," *IEEE Transactions on Robotics and Automation*, Vol. 9, No. 5, 1993, pp. 531-543.

[9]Wee, L. B. and Walker, M. W., "On the Dynamics of Contact between Space Robots and Configuration Control for Impact Minimization," *IEEE Transactions on Robotics and Automation*, Vol. 9, No. 5, 1993, pp. 581-591.

[10]Nakamura, Y. and Mukherjee, R., "Exploiting Nonholonomic Redundancy of Free-Flying Space Robots," *IEEE Transactions on Robotics and Automation*, Vol. 9, No. 4, 1993, pp. 499-506.

[11]Papadopoulos, E. and Moosavian, S. Ali A., "Dynamics & Control of Space Free-Flyers with Multiple Arms," *Journal of Advanced Robotics*, Vol. 9, No. 6, 1995, pp. 603-624.

[12]Taniwaki, S., Matunaga, S., Tsurumi, S., and Ohkami, Y., "Coordinated control of a satellite-mounted manipulator with consideration of payload Flexibility," *Journal of Control Engineering Practice*, Vol. 9, No. 2, 2001, pp. 207-215

[13]Rutkovsky, V.Y., Sukhanov, V.M., Glumov, V.M., Zemlyakov, S.D., and Dodds S.D., "Computer simulation of an adaptive control system for a free-flying space robotic module with flexible payload's transportation," *Journal of Mathematics and Computers in Simulation*, Vol. 58, No. 3, 2002, pp. 407–421.

[14]Inaba, N., Nishimaki, T., Asano, M., and Oda, M., "Rescuing a stranded satellite in space-Experimental study of satellite captures using a space manipulator," *Proc. Of IEEE/RSJ Int. Conf. on Intelligent Robots and Systems*, Las Vegas, Nevada, 2003.

[15]Yoshida, K. and Nakanishi, H. "Impedance Matching in Capturing a Satellite by a Space Robot," *IEEE/RSJ Int. Conf. on Intelligent Robots and Systems*, Las Vegas, Nevada, 2003.

[16]Raibert, M. H. and Craig, J. J., "Hybrid position/force control of manipulators," *ASME Journal of Dynamic Systems, Measurement & Control*, Vol. 126, No. 2, 1981, pp. 126-133.

[17]Hayati, S., "Hybrid position/force control of multi-arm cooperating robots," *Proc. Of the IEEE Int. Conf. On Robotics and Automation*, San Francisco, 1986, pp. 82-89.

[18]Hogan, N., "Impedance control: An approach to manipulation," *ASME Journal of Dynamic Systems, Measurement & Control*, Vol. 107, No. 1, 1985, pp. 1-24.

[19]Goldenberg, A. A., "Implementation of Force and Impedance Control in Robot Manipulators," *Proc. of the IEEE Int. Conf. on Robotics and Automation*, Philadelphia, Pennsylvania, 1988, pp. 1626-1632.

[20]Jung, S. and Hsia, T. C., "Stability and Convergence Analysis of Robust Adaptive Force Tracking Impedance Control of Robot Manipulators," *Proc. of the IEEE/RSJ Int. Conf. on Intelligent Robots and Systems*, Korea, Oct. 17-21, 1999.

[21]Arimoto, S., Han, H.Y., Cheah, C. C., and Kawamura, S., "Extension of impedance matching to nonlinear dynamics of robotic tasks," *Journal of Systems & Control Letters*, Vol. 36, No. 2, 1999, pp. 109-119.

[22]Caccavale, F., Chiacchio, P., and Chiaverini, S., "Task-Space Regulation of Cooperative Manipulators," Automatica, Vol. 36, 2000, pp. 879-887.

[23]Caccavale, F. and Villani, L., "An Impedance Control Strategy for Cooperative Manipulation," *Proc. of the IEEE/ASME Int. Conf. on Advanced Intelligent Mechatronics*, Como, Italy, July 8-12, 2001.

[24]Biagiotti, L., Liu, H., Hirzinger, G. and Melchiorri, C., "Cartesian Impedance Control for Dexterous Manipulation," *Proc. of IEEE/RSJ Int. Conf. on Intelligent Robots and Systems*, Las Vegas, Nevada, 2003.

[25]Ozawa, R. and Kobayashi, H., "A New Impedance Control Concept for Elastic Joint Robots," *Proc. of the IEEE Int. Conf. on Robotics and Automation*, Taiwan, 2003.

[26]Schneider, S. A. and Cannon, R. H., "Object Impedance Control for Cooperative Manipulation: Theory and Experimental Results," *IEEE Transactions on Robotics and Automation*, Vol. 8, No. 3, 1992, pp. 383-394.

[27]Meer, D. W. and Rock, S. M., "Coupled System Stability of Flexible-Object Impedance Control," *Proc. of the IEEE Int. Conf. on Robotics and Automation*, Nagoya, Japan, 1995, pp. 1839-1845.

[28]Moosavian, S. Ali A. and Papadopoulos, E., "On the Control of Space Free-Flyers Using Multiple Impedance Control," *Proc. of the IEEE Int. Conf. on Robotics and Automation*, NM, USA, April 21-27, 1997.

[29]Moosavian, S. Ali A. and Papadopoulos, E., "Multiple Impedance Control for Object Manipulation," *Proc. of IEEE/RSJ Int. Conf. on Intelligent Robots and Systems*, Victoria, Canada, October 13-17, 1998.

[30]Moosavian, S. Ali A. and Papadopoulos, E., "Explicit Dynamics of Space Free-Flyers with Multiple Manipulators via SPACEMAPL," *Journal of Advanced Robotics*, Vol. 18, No. 2, 2004, pp. 223-244.

[31]Meirovitch, L., *Methods of Analytical Dynamics*, McGraw-Hill, NY, 1970.

[32]Moosavian, S. Ali A. and Rastegari, R., "Force Tracking in Multiple Impedance Control of Space Free-Flyers," *Proc. of IEEE/RSJ Int. Conf. on Intelligent Robots and Systems*, Japan, 2000.

[33]Moosavian, S. Ali A. and Rastegari, R., "Disturbance Rejection Analysis of Multiple Impedance Control for Space Free-Flying Robots," *Proc. of IEEE/RSJ Int. Conf. on Intelligent Robots and Systems*, Switzerland, 2002

[34]Craig, J., *Introduction to Robotics, Mechanics and Control*, Addison Wesley, MA, 1989.

[35]De Fazio, T. L., Seltzer, D. S., and Whitney, D. E., "The Instrumented Remote Centre Compliance," *Journal of The Industrial Robot*, Vol. 11, No. 4, 1984, pp. 238-242.

Appendix

The initial conditions and parameters for the simulated system, as depicted in Figure 3, are summarized here. The SFFR parameters are described in tables 1, 2 and 3. The initial conditions are chosen as

$$\mathbf{q} = \left(x_{cm_S}, y_{cm_S}, \delta_0, \theta_{11}, \theta_{12}, \theta_{21}, \theta_{22}, \theta_{31}, \theta_{obj}\right) = (0.0, 0.0, 0.0, 2.7, -2.7, 1.0, 2.5, 0.0, 0.0) \quad (m, rad)$$
$$\dot{\mathbf{q}} = \mathbf{0}$$

The stiffness and damping properties of the RCC unit are chosen as follows, see Ref.[35], where it is assumed that it is initially free of tension or compression.

$$\mathbf{k}_e = diag(1.2, 1.2) \times 10^3 \ kg\ s^{-1}$$
$$\mathbf{b}_e = diag(5, 5) \times 10^2 \ kg\ s^{-2}$$

Table 1: The base Parameters and Saturation limits.

$\mathbf{r}_0^{(1)}$ (m)	$\mathbf{r}_0^{(2)}$ (m)	$\mathbf{r}_0^{(3)}$ (m)	$\mathbf{m}_0$ (Kg)	$\mathbf{I}_0$ (Kgm^2)	$\mathbf{F}_x$ (N)	$\mathbf{F}_y$ (N)	$\boldsymbol{\tau}_0$ (N·m)
0.5	0.5	0.5	50	10	100	100	20

Table 2: The manipulators Parameters and limits.

No	i-th body	$\mathbf{r}_i^{(m)}$ (m)	$\mathbf{l}_i^{(m)}$ (m)	$\mathbf{m}_i^{(m)}$ (Kg)	$\mathbf{I}_i^{(m)}$ (Kgm^2)	$\boldsymbol{\tau}_i^{(m)}$ (Nm)
1	1	0.50	0.50	4.0	0.50	70
1	2	0.50	0.50	3.0	0.25	70
2	1	0.50	0.50	4.0	0.50	70
2	2	0.50	0.50	3.0	0.25	70
3	1	0.25	0.25	5.0	2.00	70

Table 3: The manipulated object Parameters.

$m_o\ (Kg)$	$I_o\ (Kg \cdot m^2)$	$r_e^{(1)}(m)$	$r_e^{(2)}\ (m)$
3.0	0.5	0.2	0.2